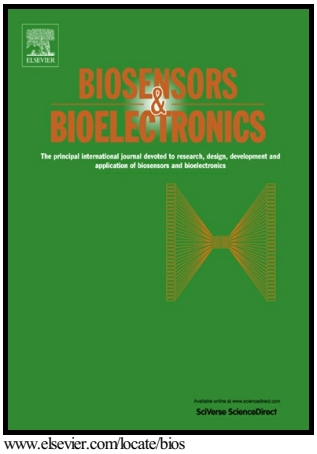

www.elsevier.com/locate/bios

Real-time monitoring of immune responses under pathogen invasion and drug interference by integrated microfluidic device coupled with worm-based biosensor

Liang Hu, Anle Ge, Xixian Wang, Shanshan Wang, Xinpei Yue, Jie Wang, Xiaojun Feng, Wei Du, Bi-Feng Liu

PII: S0956-5663(18)30243-4
DOI: https://doi.org/10.1016/j.bios.2018.03.058
Reference: BIOS10384

To appear in: *Biosensors and Bioelectronic*

Received date: 18 December 2017
Revised date: 9 March 2018
Accepted date: 27 March 2018

Cite this article as: Liang Hu, Anle Ge, Xixian Wang, Shanshan Wang, Xinpei Yue, Jie Wang, Xiaojun Feng, Wei Du and Bi-Feng Liu, Real-time monitoring of immune responses under pathogen invasion and drug interference by integrated microfluidic device coupled with worm-based biosensor, *Biosensors and Bioelectronic,* https://doi.org/10.1016/j.bios.2018.03.058

Real-time monitoring of immune responses under pathogen invasion and drug interference by integrated microfluidic device coupled with worm-based biosensor†

Liang Hu[a,b1] Anle Ge[a,c1], Xixian Wang[a,c], Shanshan Wang[a], Xinpei Yue[d], Jie Wang[a], Xiaojun Feng[a], Wei Du[a*], Bi-Feng Liu[a*]

[a] The Key Laboratory for Biomedical Photonics of MOE at Wuhan National Laboratory for Optoelectronics-Hubei Bioinformatics & Molecular Imaging Key Laboratory, Systems Biology Theme, Department of Biomedical Engineering, College of Life Science and Technology, Huazhong University of Science and Technology, Wuhan 430074, China

[b] Brain Research Center, Wuhan Institute of Physics and Mathematics, Chinese Academy of Sciences, Wuhan 430071, China

[c] Single Cell Center, CAS Key Laboratory of Biofuels and Shandong Key Laboratory of Energy Genetics, Qingdao Institute of Bioenergy and Bioprocess Technology, Chinese Academy of Sciences, Qingdao, Shandong, 266101, China

[d] School of Chemistry, Chemical engineering and Life Sciences, Wuhan University of Technology, Wuhan 430070, China

Dr. Wei Du, Email: weidu@mail.hust.edu.cn

Dr. Bi-Feng Liu, Email: bfliu@mail.hust.edu.cn

*Corresponding author. Tel: +86-27-87793180

*Corresponding author. Tel: +86-27-87792203

†Electronic Supplementary Information (ESI) available: Supplementary figures and movies.

Abstract

[1] These authors contributed equally.

Immune response to environmental pathogen invasion is a complex process to prevent host from further damage. For quantitatively understanding immune responses and revealing the pathogenic environmental information, real-time monitoring of such a whole dynamic process with single-animal resolution in well-defined environments is highly desired. In this work, an integrated microfluidic device coupled with worm-based biosensor was proposed for *in vivo* studies of dynamic immune responses and antibiotics interference in infected *C. elegans*. Individual worms housed in chambers were exposed to the various pathogens and discontinuously manipulated for imaging with limited influence on physiological activities. The expression of immune responses gene (*irg-1*) was time-lapse measured in intact worms during pathogen infection. Results demonstrated that *irg-1* gene could be induced in the presence of *P. aeruginosa* strain PA14 in a dose-dependent manner, and the survival of infected worm could be rescued under gentamicin or erythromycin treatments. We expect it to be a versatile platform to facilitate future studies on pathogenesis researches and rapid drug screen using *C. elegans* disease model.

Keywords: microfluidic chip; worm-based biosensor; immune responses; *in vivo* analysis; drug evaluation

1. Introduction

Metazoan organisms including vertebrates (such as human) and invertebrates (and even plants, to some extent) rely exclusively on the innate immune mechanisms in their responses against pathogens (Gravato-Nobre and Hodgkin, 2005). Epithelial cells from organs such as the skin and the intestine provide major routes of entry for intracellular pathogens (Gallo and Hooper, 2012). The evolved complex immune responses in these cells depend on the recognition and subsequent elimination of pathogens by genomically ‘hard-wired’ mechanisms (Gravato-Nobre and Hodgkin, 2005). Thus, visualizing and monitoring the infection process *in vivo* can facilitate understanding how the animals discriminate pathogens from nonpathogens.

The soil nematode *Caenorhabditis elegans* (*C. elegans*), which have long

considered as biosensors of stress responses to environmental toxics (Peter et al. 1996; McLaggan et al. 2012), have also emerged as an ideal model host for microbial pathogenesis and innate immunity studies, benefiting from its advantages of low cost, simple maintenance, short life cycle, as well as optical accessibility for *in vivo* analysis (Balla and Troemel, 2013; Ermolaeva and Schumacher, 2014; Kurz and Ewbank, 2003; Sifri et al., 2003). *C. elegans* feed on bacteria but are susceptible to infections by pathogens in its natural environment. Growing evidences showed that pathogens such as *Pseudomonas aeruginosa* and *Staphylococcus aureus* can invade worm's intestinal cells, trigger specific innate immunity defenses and even cause the disease of intestinal distention and lysis, leading to worm death in a short period (Irazoqui et al., 2010; Rajamuthiah et al., 2014). More importantly, this increasing list of infectious microbes, including different bacteria and fungus that can elicit significant host responses in worm, are usually known to cause human diseases and of clinical interest (Ewbank and Zugasti, 2011).

Studies of immune responses in *C. elegans* have been generally performed by using genetic and environmental manipulations on agar plates. These conventional methods allow for the detection of genetic immunomodulation, microbial virulence and antibacterial drug effect by monitoring behavioral changes, survival rate and gene expression of worms (Arvanitis et al., 2013; Dunbar et al., 2012; Kim, 2013; Moy et al., 2006; Tan et al., 1999). However, such open-field culture methods rely on glue or anesthesia for immobilization while imaging, lacking the capability to provide a controllable pathogenic environment and monitor the dynamic physiological changes throughout the long-term process on a single worm. In addition, manual manipulation of worms is time-consuming, labor-intensive and easy to cause worms losing (Lee et al., 2016).

For the purpose of observing *C. elegans* in a well-controlled environment, microfluidic tools have been developed with extended applications, such as worm sorting (Aubry et al., 2015; Wang et al., 2015; Yan et al., 2016), behavioral dynamics (Albrecht and Bargmann, 2011; Aubry and Lu, 2017; Hu et al., 2015b), neuronal imaging (Chokshi et al., 2010; Chronis et al., 2007; Hu et al., 2015a; Hu et al., 2016;

Schrodel et al., 2013; Wang et al., 2011; Wang et al., 2013a) and microsurgery (Gokce et al., 2017; Gonzales et al., 2017; Samara et al., 2010; Zhao et al., 2013). The biocompatible microfluidic systems enable the researchers to handle worms meanwhile perform *in vivo* analysis (Cornaglia et al., 2017; Crane et al., 2010; San-Miguel and Lu, 2013). In previous studies, microfluidic infection assays have been used for co-culturing worm with various microbes. Zhang et al. demonstrated a microfluidic four-choice maze assay for the test of olfactory preference to pathogenic bacteria in *C. elegans* (Zhang et al. 2005). Yang et al. proposed an integrated microfluidic platform allowing *S. aureus* infection and anti-infection agent screening to be performed *in vivo* (Yang et al., 2013). In these works, immune responses were evaluated by worms' behaviors or survival rates. To measure molecular kinetics of immune process, an on-chip assay was reported for long-term tracking on worm population (Lee et al. 2016). However, gaining quantitative understanding of immune defenses in an individual worm is currently limited, owing to the lack of manner for precise capturing and dynamic monitoring of these living tiny animals.

Here we proposed an integrated microfluidic device coupled with worm-based biosensor for *in vivo* analysis of dynamic immune responses and antibiotics evaluation with single-worm resolution. Parallel chambers connected with a tree-like delivery system were used to house *C. elegans* individually and carry out infection assays without cross-interference. Worm chamber covered with pneumatic micro-valve was modified to enable discontinuous immobilization with limited physiological influence and high-throughput, allowing long-term and real-time monitoring of immune responses. We performed the pathogen infection on single worms with pathogenic *P. aeruginosa* strain PA14, which can specifically induce *infection response gene 1* (*irg-1*) expression under the mediation of bZIP transcription factor *zip-2* (Estes et al., 2010). Time-lapse measurements of *irg::GFP* indicated a dose-dependent infection during pathogen infection, as well as reveal the information of the pathogenic environments to which worm was exposed. Moreover, antimicrobial effect of antibiotics for the recovery of infected worm was tested using the established platform. Our integrated device presents a unique approach for investigating

dynamical biological processes *in vivo*, and is expected to be a reliable, rapid system for antibacterial drug test.

2. Materials and methods

1.1. Chemicals and reagents

Reagents of analytical grade including NaCl, NaOH, Tris-HCl, KCl, $MgSO_4$, $CaCl_2$, NaClO, fluorescein and trimethylchlorosilane were purchased from Sinopharm Chemical Reagent (Shanghai, China). Erythromycin was purchased from Aladdin (Shanghai, China) and gentamycin was from Tongji Hospital (Wuhan, China). Agar power, peptone, cholesterin, yeast extract, tryptone, fluorescein sodium salt and Pluronic F127 were purchased from Sigma-Aldrich (MO, USA). SU-8^{TM} (GM1070) was purchased from Gersteltec Sarl (Switzerland) and Ploy-dimethysiloxane (PDMS, Sylgard 184) with curing agent were purchased from Dow Corning (MI, USA). Water used for all the solutions preparation was purified by the Direct-Q system (Millipore, MA, USA). Pluronic F-127 solution was prepared by diluting 5% (weight/volume) Pluronic F-127 in M13 buffer. All solutions were sterilized by filtration (0.22 μm microporous membrane filter) or autoclave (121 °C, 20 min) before use.

1.2. Worm strains and Bacterial strains

AU133 *agls17* (*irg-1::gfp*) and the deletion allele ERT012 *zip-2 (tm4067)* were kindly provided by Dr. Emily R. Troemel (UC San Diego, CA, USA). TJ356 *zls356* (*daf-16::gfp, rol-6*) were obtained from the Caenorhabditis Genetics Centre (CGC) at the University of Minnesota (St. Paul). The worm strains were grown at 20℃ on nematode growth medium (NGM) ager plates seeded with *E. coli* OP50 as previously described (Stiernagle, 2006). Worms were synchronized prior to assay for ensuring the experimental consistency.

P. aeruginosa strain PA14 was kindly provided by Dr. Kun Zhu (Institute of

Microbiology, Chinese Academy of Sciences, Beijing, China). *S. aureus* was donated by the Institute of Environmental Resource & Microbial Technology (Huazhong University of Science and Technology, Wuhan, China). *E. coli* strain OP50 and transgenic strain BL21 (DE3) bacteria expressing the green fluorescent protein were maintained in our own lab.

For infection assay, the standard protocols were followed from the literature (Zhang et al., 2005). Briefly, a single PA14 or OP50 colony was inoculated in LB medium (10.0 g of tryptone, 5.0 g of yeast extract and 5.0 g of NaCl to 1.0 litre of distilled water) and shaken overnight at 37 °C. For chip based infection assay, the saturated PA14 solution (OD_{600}=1.6) or OP50 solution (OD_{600}=0.9) were centrifuged and re-suspended in M13 buffer (30 mM Tris, 100 mM NaCl, 10 mM KCl, pH 7.2) to obtain a final concentration of 10^9 cells mL^{-1}. After loading worms into the microfluidic device, the bacterial suspension was delivered into the device at a rate of 1 μL min^{-1}.

1.3. Chip design and fabrication

A two-layer microfluidic chip was designed for co-culturing *C. elegans* with various pathogenic bacteria while allowing long-term monitoring the immune responses and evaluating the antibiotic effect of antibiotics simultaneously. As shown in Fig. 1, the bottom layer (colored blue) contain 8 array chambers for worm culture (80 μm height, 500 μm width and 5 mm length), which is connected with independent worm loading channels (40 μm height) and a tree-like bacteria/drug delivery system (80 μm height). The top layer (colored green) containing a curve-shaped pneumatic valve (20 μm in height) for immobilizing the worms in bottom chambers.

The two-layer PDMS microfluidic chip was fabricated according to standard soft lithography and rapid prototyping (Whitesides et al., 2001). Briefly, SU-8™ molds were fabricated on 3.5-inch silicon wafers using standard soft lithography technique. The PDMS layers were fabricated by pouring a mixture of PDMS and curing agent at a mass ratio of 10:1 for top layer and 20:1 for bottom layer onto the SU-8 molds. After curing at 65 °C for 4 h, the top layer was peeled off, aligned and irreversibly

bonded to the bottom layer after oxygen plasma treatment, forming a PDMS membrane (20 μm thick) between worm channels and upper valve. Finally, the bonded PDMS layer was peeled off from the silicon substrate and bonded to a glass coverslip treated by oxygen plasma to form the final device. Punching process was performed before each plasma treatment.

1.4. Worm manipulation and imaging on chip

Young adult worm suspended in the M13 buffer is loaded via individual inlet and squeezed into worm chamber through a wedge channel. After being housed in culture chamber, the worm was not allowed to escape from the chamber, owing to the limited size of loading microchannel and the narrow grooves in delivery microchannel (Fig. 1). Afterwards, various concentrations of bacteria were delivered to culture and infect worms. To confine the worm for fluorescence imaging, the pneumatic valve was switched on by increasing the air actuating pressure (30 MPa) of the control layer (Fig. 2A). The deformable PDMS membrane is then pushed down to squeeze the worms to the side of the chamber in order to reduce the activities of free-moving worms. Worms keep in a "static" state until the end of image acquisition and recover rapidly as soon as release.

For monitoring *irg-1::GFP* induction *in vivo*, an inverted fluorescence microscope (IX 71, Olympus, Japan) was used for time lapse fluorescence imaging . Optical imaging of GFP was realized using a fluorescent filter (472/30 nm excitation; 495 nm dichroic mirror; 520/35 nm emission, U-MF2, Olympus, Japan). For tracing *irg-1::GFP*, image data was acquired every 1 or 2 hours and the image sequences were analyzed by Image-Pro Plus 6.0 software (Media Cybernetics, USA). The change of fluorescence intensity (F) relative to the basal fluorescence (F0) was calculated using the formula F/F0.

1.5. Pathogen infection and drug evaluation assays

Before each experiment, the microfluidic devices were incubated with Pluronic

F-127 solution for 30 min followed by rinsing with M13 buffer. Free bacteria depositing on the surface of the PDMS could be prevented by Pluronic solution that is a kind of surface-activating agent (Xian et al., 2013). The synchronized young adult worms were loaded into the culture chambers then incubated with different concentration of bacteria solution by the syringe pump (Harvard Apparatus, Holliston, MA) at 20 °C. The worms were judged as dead when they did not swim in response to the change of fluid flow rate in the microchannels. The killing curve of each group was calculated according to the survival rate of the trapped worms every 12 hours.

3. Results and discussion

3.1 *Evaluation of the microfluidic system*

Considering the long-term culture and maintenance of worms in chip, feeding behaviors and motilities were first evaluated. The loaded worm was confined in an individual culture chamber without escaping, which was ensured by its free swim without disturbing food ingestion (Fig. S1). Body bends were often used as an easily quantified parameter of worms' motion (Kerr et al., 2011). We measured the bending frequency and the result showed a relative high physiological activity of the worm over time in chip (Fig. 2). For dynamic imaging in an individual worm, pneumatic valves with deformable membrane were designed to immobilize worm reversibly. However, the spindle-shaped and smooth body of worm makes it easy to escape from the restricted area when applied with a pressured membrane for immobilization. To improve the successful rate of immobilization, we modified the culture chamber wall with slight curved edge, which could help distributing a uniform pressure at the edge of chamber while the PDMS membrane encounters large deformation. Free-moving animal was locked at the edge area of the chamber immediately without considering its previous location (Fig. 2 and movie S1), and the results showed a high capture rate of more than 90%.

Although the worm was successfully restricted in a "static" state, the crowded space and deformed membrane still might induce stress responses in the worm (Wang

et al., 2013b). To address this question, nuclear localization of DAF-16 was observed to monitor physiological responses of the worm during immobilization process by using the TJ356 strain expressing *DAF-16::GFP*. As shown in Fig. 2, no significant nuclear localization was induced under the actuating pressure of 0.03 and 0.06 MPa in 10 minutes, respectively. Actually, fluorescence imaging and release of worm was performed within 1 minute under the pressure of 0.03 MPa during the experimental process of immobilization, indicating a negligible DAF-16-mediated stress response in *C. elegans.* Above results demonstrated the capability of our device to discontinuously manipulate individual worm with minimum physiological influence.

3.2 *Quantitative measurements of irg-1::GFP induction in C. elegans*

C. elegans can protect itself from pathogenic infections by quickly setting off innate immune responses. *P. aeruginosa* is one of the well-characterized human opportunistic pathogens that can cause death in cystic fibrosis patients. Particular *P. aeruginosa* strain like PA14 has been reported to invade worm intestine cells and shorten its lifespan (Cezairliyan et al., 2013; Mahajan-Miklos et al., 1999). Previous works also indicated that worms respond to PA14 infection mainly involved in a bZIP transcription factor *zip-2*-mediated induction of PMK-1-independent genes *irg-1* (Dunbar et al., 2012; Estes et al., 2010). We first measured the immune responses of wild-type nematode to *E. coli*, *S. aureus* as well as *P. aeruginosa* PA14 using transgenic animals containing the *irg-1::GFP* fusion. Enhanced GFP expression was showed in intestine cells when fed with PA14 after 12 hours post infection (hpi), but very little change with other pathogenic and non-pathogenic bacteria (Fig. S2), consisting with previous reports that *irg-1::GFP* is specifically induced by virulent *P. aeruginosa* PA14. The observation of PA14-induced *irg-1* up-regulation makes it a reliable infection model for immune studies.

To further clarify the dynamic changes of *irg-1::GFP* over time in an intact worm, one should allow the worm to move freely for food ingestion and also to keep motionless for real-time imaging. Our microfluidic system provided a unique opportunity to obtain time-lapse imaging in the same worm, which was not

convenient in agar-based method. Fluorescent images of confined worm were captured once every hour and the ratio change of GFP was measured quantitatively. A significant increase of *irg-1::GFP* with apparent "S" curve was observed in intestine cells of wild-type animals (Fig. 3). Rapid elevation of fluorescent signals initiated at 4 hpi and ended to a saturation level after 10 hours treatment. By contrast, *irg-1::GFP* in worm mutant with deletion of allele *zip-2* failed to respond to PA14 (Fig. 3), indicating the important role of *zip-2* for immune defense against PA14 infection. *In vivo* results demonstrated that the established microfluidic system was capable of real-time monitoring the immune responses in an intact worm.

2.

2.1.

2.2.

2.3. Application of the device for various bacterial infection

Hazardous food can cause visceral malaise after ingestion, requiring animal to learn to modify its food preference for enhancing survival in complex natural environment. In most of previous works, infection assays were usually performed on worm population treated with single food. To better understand how an individual worm chose the food with high quality from others, our device was further adopted to monitor *in vivo* immune responses to mixtures of *E. coli* OP50 and *P. aeruginosa* PA14 in a complementary way. Mixtures with a serial of volume ratio (100% PA14, 67% PA14 and 33% OP50, 33% PA14 and 67% OP50, 100% OP50, respectively) were on-line prepared and delivered to the isolated worm chambers. Time course of the *irg-1::GFP* induction was shown in Fig. 4A. Comparing to the treatment of PA14, rise of GFP signals slowed down as the mixing ratio of OP50 increasing and showed a weak decline in the absence of PA14, revealing a dose-dependent infection of pathogens. Moreover, *irg-1::GFP* induction in two OP50/PA14 mixture groups climbed to a same level which was lower than that in PA14-only group (Fig. 4B). The distribution of *irg-1* expression significantly broadened over time in 100% PA14 treatment group in comparison with the groups with OP50, suggesting that the

individual difference of worms during pathogen invasion. In fact, *E. coli* OP50 could not induce the *irg-1::GFP* change in neither WT nor *zip-2* mutant animals (Fig. S3), indicating that OP50 is an ideal food in worm's food preference behaviors. In addition，PA14 with low concentration (about 10^7 cells mL^{-1}, lower than 10% PA14) failed to trigger worms' immune response of *irg-1*. These results of our research could provide an explanation for previous reporting that *C. elegans* can learn to avoid the pathogenic bacteria after several hours interacting with the pathogen whose odour was even more attractive to worms (Zhang et al. 2005).

2.4. Application of the device for drug evaluation

C. elegans is considered as a disease model not only for revealing disease mechanisms, but also for high-throughput drug evaluation (Arvanitis et al. 2013; Ewbank and Zugasti 2011). Thus, the proposed platform was further validated the capability in measuring and comparing concentration-dependent recovery effect of antibiotics in infected worms. In this work, two antibiotics of gentamicin (GM) and erythromycin (EM) were chosen as model compounds for treatments of PA14 infected worms. GM is responsible for a wide range of nosocomial infections such as pneumonia and bacteremia, as well as able to effectively inhibit the growth of *P. aeruginosa* with the increase of concentration (Dai et al. 2013). EM, a broad-spectrum antibiotic, is reported to inhibit extracellular production of elastase of *P. aeruginosa* without affecting the proliferation of the bacteria, and the low-dose long-term EM therapy demonstrated the potential of reduction in bacterial biofilm formation (Nagata et al. 2004; Sakata et al. 1993).

Antibiotic treatments were performed after exposing worms to pathogen PA14 infections for 12-16 hours, according to the results of infection assays. Antibiotics were prepared in M13 buffer with OP50 used as a food source to promote the drug uptake in such a liquid condition. In GM therapy group, the expression of *irg-1::GFP* in infected worms peaked within 6 hours and decayed over the 18 hours when treated with low-dose GM (Fig. 5A). In contrast, a continued decrease in *irg-1::GFP* signals was observed under high-level GM (400 mg L^{-1}) treatment. We further monitored the

lifespan of the infected worms after GM therapy. Survival rate was counted every 12 hours and the average lifespan of *C. elegans* was also scored. It was observed that worms fed on PA14 would die within 5 days, but could be rescued to varying degrees by treated with different levels of GM (Fig. 5C). Interestingly, the extended lifespans of infected worm were observed in groups of 40 and 400 mg L^{-1} GM treatments, but not in 100 and 200 mg L^{-1} groups, showing a dose-independent manner (Fig. S4 and Fig. 5D). In EM therapy group, significant increase in *irg-1::GFP* was observed in low-dose EM therapy (40 mg L^{-1}), and higher dose of drugs showed weaker antibiotic effect on host survival (Fig. 5C and 5D). In addition, the behavior of laying egg was observed to be blocked in infected worms even treated with antibiotics (Fig. S5), indicating irreversible damage on vulva was caused by PA14. Taken together, our proposed microfluidic system was confirmed to concurrently investigate microbial pathogenesis and drug therapy in intact worms.

3. Conclusion

In this work, we have developed an integrated microfluidic device coupled with worm-based biosensor for *in vivo* monitoring the dynamics of immune responses upon pathogen invasion and antibiotics interference at single-worm resolution. Comparing to the glue- or anesthesia-based approaches for worm imaging in agar plates, the proposed micro system provided a reliable way to discontinuously confine an individual animal for whole-process tracking under a normal physiological situation. The modified chamber structure also enhanced the success rate of worm capture, allowing rapid immobilization, imaging and release of worm to be performed within 1 minute. A tree-like delivery system was connected to parallel worm chambers for infection assay individually. Induction dynamics of *irg-1* gene in intestine cells of wild-type and *zip-2* mutant worms were simultaneously monitored *in vivo* when treated with *P. aeruginosa* PA14. Quantitative measurements of *irg-1::GFP* showed strong induction with “S” curve over time by PA14 but blocking in *zip-2* worm mutant. *irg-1* responses also showed significant dose-dependent when exposed to various mixtures of PA14 and *E. coli* OP50. Furthermore, the platform was applied

in evaluating the recovery of infected worms after antibiotics treatments. Overall, the integrated, easy-to-handle and all-inclusive microfluidic system coupled with novel worm-based biosensor would be useful to reveal the complex pathogenic environments, facilitate pathogenesis research and rapid screening of antibiotics by using *C. elegans* disease model.

Acknowledgments

We thank Prof. Troemel for kindly providing *C. elegans* strain AU133 and ERT012; Dr. Zhu for kindly providing *P. aeruginosa* strain PA14. The authors gratefully acknowledge the financial supports from National Key R&D Program of China (2016YFF0100801), National Natural Science Foundation of China (21475049, 31471257 and 21275060), and the Fundamental Research Funds for the Central Universities (2016YXZD061).

References

Albrecht, D.R., Bargmann, C.I., 2011. Nat Methods 8(7), 599-605.

Arvanitis, M., Glavis-Bloom, J., Mylonakis, E., 2013. Curr Opin Pharmacol 13(5), 769-774.

Aubry, G., Lu, H., 2017. Lab Chip 17(24), 4303-4311.

Aubry, G., Zhan, M., Lu, H., 2015. Lab Chip 15(6), 1424-1431.

Balla, K.M., Troemel, E.R., 2013. Cell Microbiol 15(8), 1313-1322.

Cezairliyan, B., Vinayavekhin, N., Grenfell-Lee, D., Yuen, G.J., Saghatelian, A., Ausubel, F.M., 2013. Plos Pathog 9(1), e1003101.

Chokshi, T.V., Bazopoulou, D., Chronis, N., 2010. Lab Chip 10(20), 2758-2763.

Chronis, N., Zimmer, M., Bargmann, C.I., 2007. Nat Methods 4(9), 727-731.

Cornaglia, M., Lehnert, T., Gijs, M.A.M., 2017. Lab Chip 17(22), 3736-3759.

Crane, M.M., Chung, K., Stirman, J., Lu, H., 2010. Lab Chip 10(12), 1509-1517.

Dai, J., Yoon, S.H., Sim, H.Y., Yang, Y.S., Oh, T.K., Kim, J.F., Hong, J.W., 2013. Anal Chem 85(12), 5892-5899.

Dunbar, T.L., Yan, Z., Balla, K.M., Smelkinson, M.G., Troemel, E.R., 2012. Cell Host Microbe 11(4), 375-386.

Ermolaeva, M.A., Schumacher, B., 2014. Semin Immunol 26(4), 303-309.

Estes, K.A., Dunbar, T.L., Powell, J.R., Ausubel, F.M., Troemel, E.R., 2010. P Natl Acad Sci USA 107(5), 2153-2158.

Ewbank, J.J., Zugasti, O., 2011. Dis Model Mech 4(3), 300-304.

Gallo, R.L., Hooper, L.V., 2012. Nat Rev Immunol 12(7), 503-516.

Gokce, S.K., Hegarty, E.M., Mondal, S., Zhao, P., Ghorashian, N., Hilliard, M.A., Ben-Yakar, A., 2017. Sci Rep-UK 7(1), 9837.

Gonzales, D.L., Badhiwala, K.N., Vercosa, D.G., Avants, B.W., Liu, Z., Zhong, W., Robinson, J.T., 2017. Nat Nanotechnol 12(7), 684-691.

Gravato-Nobre, M.J., Hodgkin, J., 2005. Cell Microbiol 7(6), 741-751.

Hu, L., Ge, A., Wang, X., Wang, S., Gao, Y., Feng, X., Du, W., Liu, B.F., 2016. Lab Chip 16(20), 4020-4027.

Hu, L., Wang, J., Feng, X., Du, W., Liu, B.-F., 2015a. Sensor Actuat B-Chem 209(0), 109-115.

Hu, L., Ye, J.J., Tan, H.W., Ge, A., Tang, L.C., Feng, X.J., Du, W., Liu, B.F., 2015b. Anal Chim Acta 887, 155-162.

Irazoqui, J.E., Troemel, E.R., Feinbaum, R.L., Luhachack, L.G., Cezairliyan, B.O., Ausubel, F.M., 2010. Plos Pathog 6(7), e1000982.

Kerr, R.A., Swierczek, N.A., Giles, A.C., Rankin, C.H., 2011. Nat Methods 8(7), 592-598.

Kim, D.H., 2013. Annu Rev Genet 47, 233-246.

Kurz, C.L., Ewbank, J.J., 2003. Nat Rev Genet 4(5), 380-390.

Lee, K.S., Lee, L.E., Levine, E., 2016. Sci Rep-UK 6, 35862.

Mahajan-Miklos, S., Tan, M.-W., Rahme, L.G., Ausubel, F.M., 1999. Cell 96(1), 47-56.

McLaggan, D., Amezaga, M.R., Petra, E., Frost, A., Duff, E.I., Rhind, S.M., Fowler, P.A., Glover, L.A., Lagido, C., 2012. Plos One 7(10), e46503.

Moy, T.I., Ball, A.R., Anklesaria, Z., Casadei, G., Lewis, K., Ausubel, F.M., 2006. P Natl Acad Sci USA 103(27), 10414-10419.

Nagata, T., Mukae, H., Kadota, J., Hayashi, T., Fujii, T., Kuroki, M., Shirai, R., Yanagihara, K., Tomono, K., Koji, T., Kohno, S., 2004. Antimicrob Agents Ch 48(6), 2251-2259.

Peter, E., Candido, M., Jones, D., 1996. Trends Biotechnol 14(4), 125-129.

Rajamuthiah, R., Fuchs, B.B., Jayamani, E., Kim, Y., Larkins-Ford, J., Conery, A., Ausubel, F.M.,

Mylonakis, E., 2014. Plos One 9(2), e89189.

Sakata, K., Yajima, H., Tanaka, K., Sakamoto, Y., Yamamoto, K., Yoshida, A., Dohi, Y., 1993. Am Rev Respir Dis 148(4 Pt 1), 1061-1065.

Samara, C., Rohde, C.B., Gilleland, C.L., Norton, S., Haggarty, S.J., Yanik, M.F., 2010. P Natl Acad Sci USA 107(43), 18342-18347.

San-Miguel A. and Lu H., 2013. WormBook.

Schrodel, T., Prevedel, R., Aumayr, K., Zimmer, M., Vaziri, A., 2013. Nat Methods 10(10), 1013-1020.

Sifri, C.D., Begun, J., Ausubel, F.M., Calderwood, S.B., 2003. Infect Immun 71(4), 2208-2217.

Stiernagle, T., 2006. WormBook.

Tan, M.W., Mahajan-Miklos, S., Ausubel, F.M., 1999. P Natl Acad Sci USA 96(2), 715-720.

Wang, J., Feng, X., Du, W., Liu, B.F., 2011. Analytica Chimica Acta 701(1), 23-28.

Wang, J., Li, Z., Xu, Z., Hu, L., Feng, X., Chen, M., Du, W., Wu, Z., Luo, Q., Xu, T., Liu, B.F., 2013a. Sensor Actuat B-Chem 178, 343-349.

Wang, X., Hu, R., Ge, A., Hu, L., Wang, S., Feng, X., Du, W., Liu, B.F., 2015. Lab Chip 15(11), 2513-2521.

Wang, X., Tang, L., Xia, Y., Hu, L., Feng, X., Du, W., Liu, B.F., 2013b. Integr Biol-UK 5(4), 728-737.

Whitesides, G.M., Ostuni, E., Takayama, S., Jiang, X., Ingber, D.E., 2001. Annu Rev Biomed Eng 3(1), 335-373.

Xian, B., Shen, J., Chen, W., Sun, N., Qiao, N., Jiang, D., Yu, T., Men, Y., Han, Z., Pang, Y., Kaeberlein, M., Huang, Y., Han, J.-D.J., 2013. Aging Cell 12(3), 398-409.

Yan, Y., Boey, D., Ng, L.T., Gruber, J., Bettiol, A., Thakor, N.V., Chen, C.-H., 2016. Biosens Bioelectron 77, 428-434.

Yang, J., Chen, Z., 2013. Lab Chip 13(17), 3373-3382.

Zhang, Y., Lu, H., Bargmann, C.I., 2005. Nature 438(7065), 179-184.

Zhao, X., Xu, F., Tang, L., Du, W., Feng, X., Liu, B.-F., 2013. Biosens Bioelectron 50, 28-34.

Figure captions:

Fig. 1 Schematic diagram of the microfluidic device. Two-layer microfluidic chip was designed for worm culture and immobilization. Enlarged view showed the wedge-shaped worm loading channel with 40 μm height.

Fig. 2 Evaluations of the microfluidic system for manipulating worm under normal physiological situation. (A) Free-moving worm (i) could be immobilized (ii) and released reversibly and kept high physiological activities over 24 hours in chip chamber (B). Error bar indicated standard error of the mean (SEM), n = 4. (C) No significant stress response was observed in *C. elegans* by analyzing DAF-16 nuclear localization after immobilization for 10 min under the actuator pressure of 0.03 and 0.06 MPa. Scale bar, 50 μm.

Fig. 3 (A) Representative of *irg-1::GFP* induction in respond to PA14 in wild-type and *zip-2* mutant animals. Images were captured every 1 hour. Scale bar, 80 μm. (B) Measurements of fluorescence intensity of *irg-1* (WT, n = 16; *zip-2*, n = 8). Worms were exposed to PA14 at 0 hour.

Fig. 4 (A) *irg-1* induction in respond to mixtures of PA14 and OP50. (B) Comparison of saturation values of relative fluorescence intensity in groups of A. Each group was repeated 3 times and the error bars indicated SEM. The statistical significances of differences in peak value between each two groups are indicated (* $p < 0.05$, ** $p < 0.01$, N.S. denote no significant difference, student's t-test).

Fig. 5 Antibiotics evaluation in infected worms. Fluorescence intensity changes of

irg-1::GFP when treated with various concentrations of antibiotic GM (A) and EM (B). The survival rate (C) and the average lifespans (D) of the infected worms after treatment with antibiotics. 20±5 worms were used in each trial and error bar indicated SEM. The statistical significant difference in average lifespan compared to the mock group was tested by t-test (* $p < 0.05$, ** $p < 0.01$).

Video S1 : "Time-lapse imaging of worm immobilization and release using pneumatic valve".

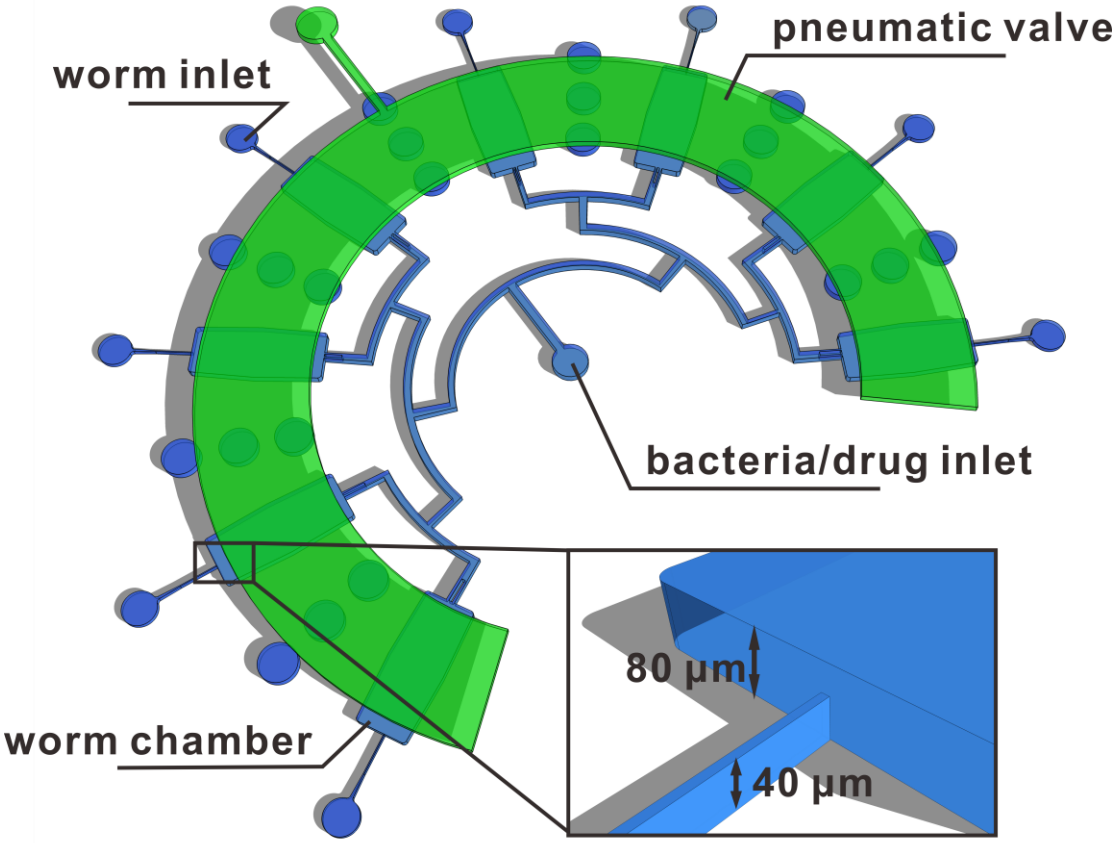

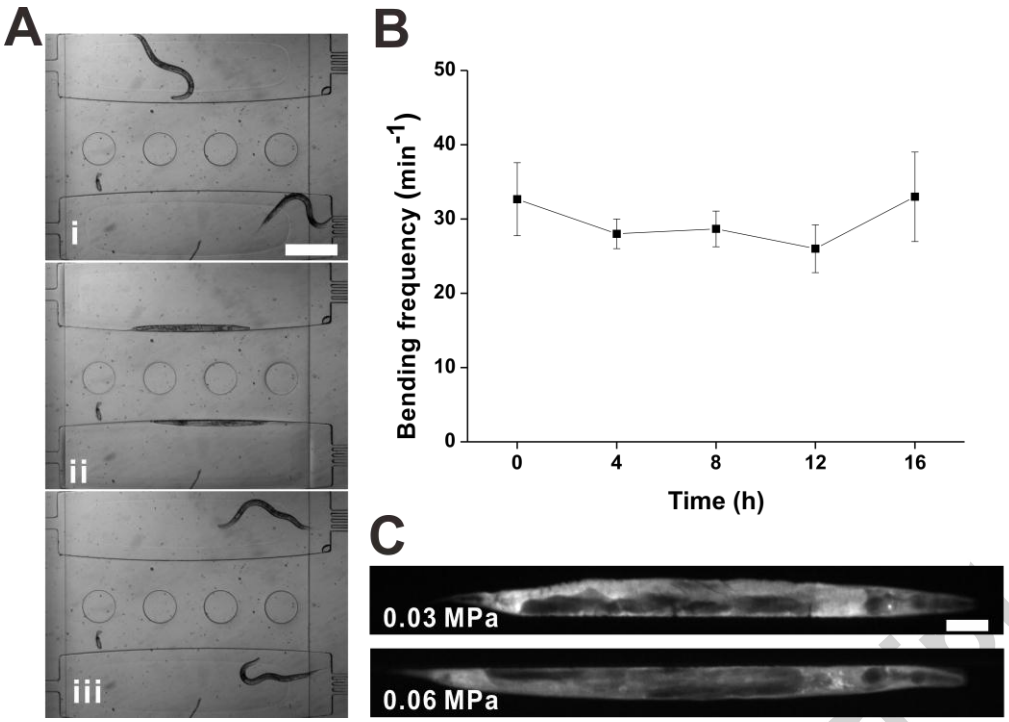

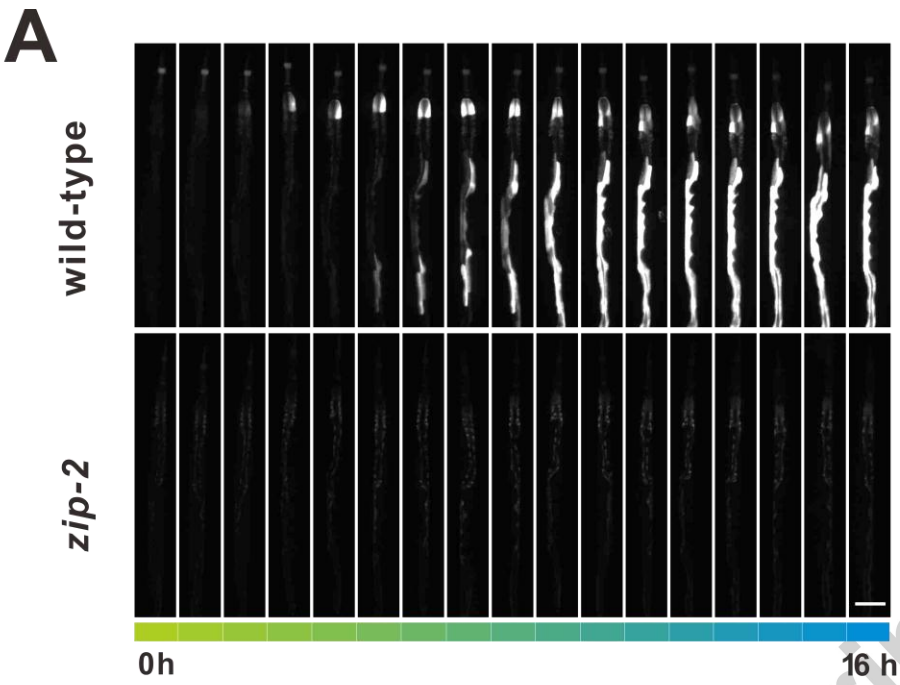

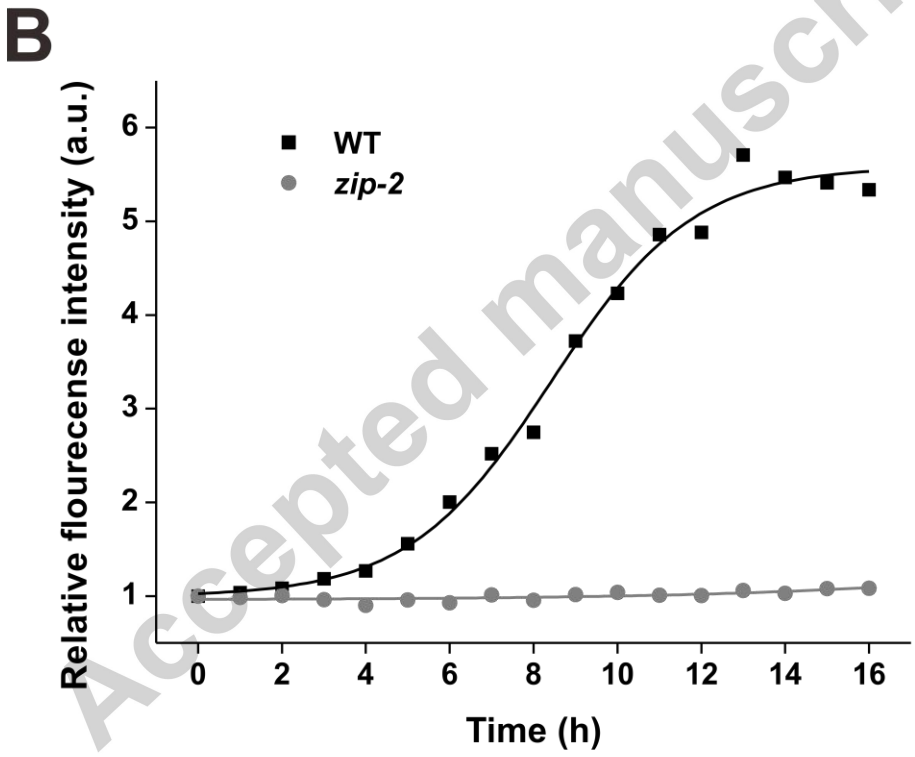

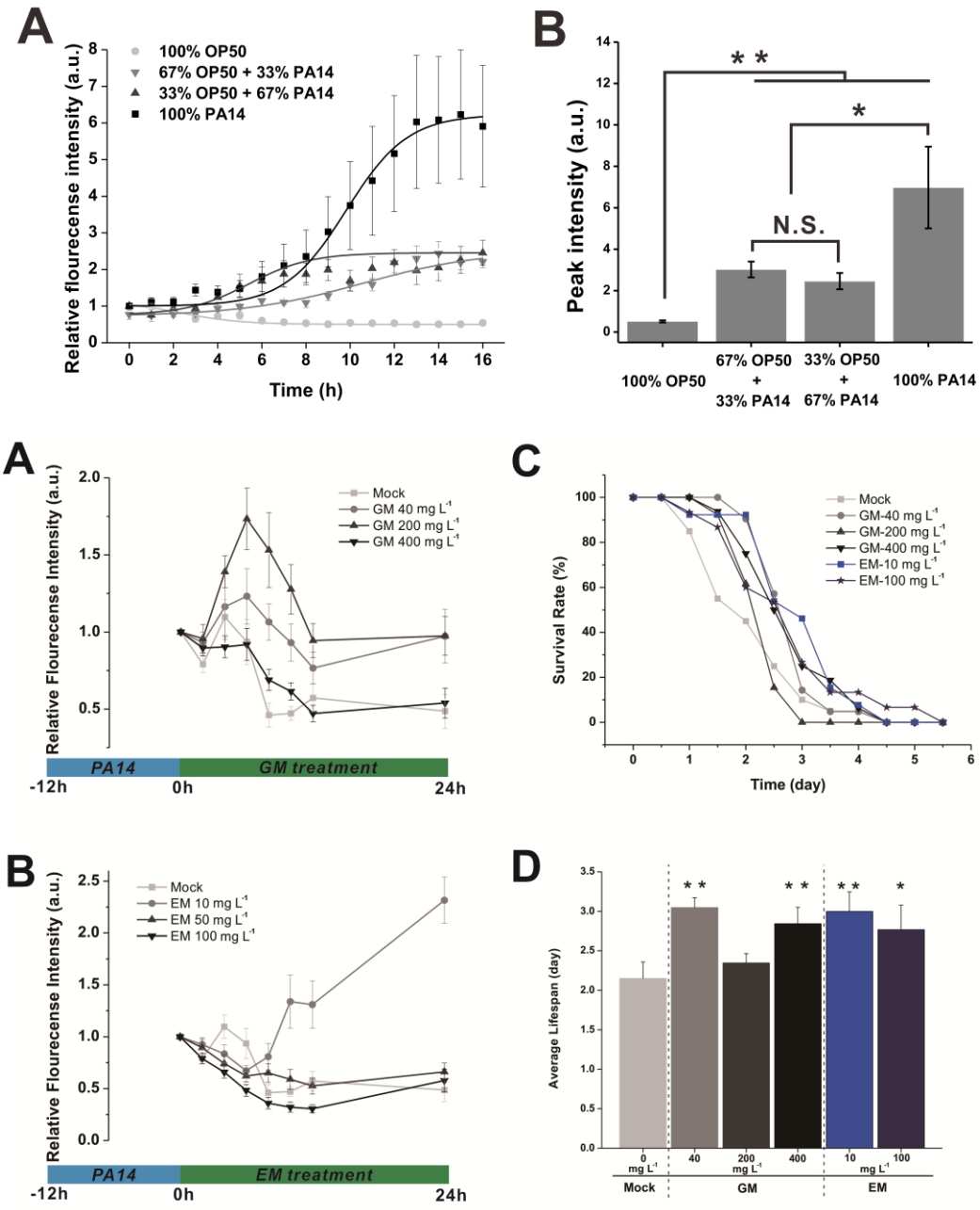

Highlights

- An integrated microfluidic device coupled with worm-based biosensor for quantitative analysis with single-animal resolution.
- Dynamic monitoring of immune responses facilitate pathogenic studies and help revealing the pathogenic environmental information.
- Antibiotics evaluation could be performed by using the *C. elegans* infection model in microfluidic chip.